NONLINEAR OPTICAL PHENOMENA

PACS numbers: 42.65.Dr; 42.70.Mp; 63.20.–e
DOI: 10.1070/QE2011v041n04ABEH014527

Spontaneous and stimulated Raman scattering in $ZnWO_4$ crystals

T.T. Basiev, A.Ya. Karasik, A.A. Sobol, D.S. Chunaev, V.E. Shukshin

Abstract. **Spontaneous and stimulated Raman scattering (SRS) are studied in $ZnWO_4$ crystals with a wolframite structure. The polarised Raman scattering spectra corresponding to all the six independent Raman tensor components are measured. The frequencies of the complete set of vibrational modes are identified. The threshold pump energies for SRS in $ZnWO_4$ and $KGd(WO_4)_2$ crystals are measured upon excitation by picosecond 1047-nm pulses of a Nd : YLF laser. The SRS gains for $ZnWO_4$ crystals are determined based on the measured thresholds and spectroscopic parameters of the crystals.**

Keywords: *Raman spectroscopy, $ZnWO_4$, stimulated Raman scattering*.

1. Introduction

The $MeWO_4$ (Me = Ca, Sr, Ba, Pb, Zn) crystals with scheelite and wolframite structures are widely used for creating frequency converters based on stimulated Raman scattering (SRS) and as detectors of ionising radiation [1 – 3]. Each of these crystals has a wide set of vibrational resonances and corresponding narrow lines in the Raman spectra with the Stokes shifts from 10 to ~ 1000 cm^{-1}. Compared to the crystals formed by oxyanion complexes [CO_3], [NO_3], and [PO_4], tungstate crystals have more intense Raman lines and, hence, higher Raman gains. Advantages of tungstate crystals include a wide transparency window in the visible and near-IR spectral regions and a high hardness, heat conduction, and moisture resistance. Among the mentioned crystals, zinc tungstate is the crystal whose nonlinear properties are studied in less detail. The aim of this work is to study the spontaneous and stimulated Raman scattering in the $ZnWO_4$ crystal and compare its SRS gain parameters with the parameters of the well-known $KGd(WO_4)_2$ (KGW) crystal.

T.T. Basiev, A.Ya. Karasik, A.A. Sobol, D.S. Chunaev, V.E. Shukshin
A.M. Prokhorov General Physics Institute, Russian Academy of Sciences, ul. Vavilova 38, 119991 Moscow, Russia;
e-mail: chunaev_d@lst.gpi.ru, shukshinve@lst.gpi.ru

Received 28 December 2010
Kvantovaya Elektronika **41** (4) 370 – 372 (2011)
Translated by M.N. Basieva

2. Raman spectroscopy

$ZnWO_4$ crystals have a wolframite structure with the monoclinic space group P2/c (C_{2h}^4) and two formula units per unit cell [4].

According to the theoretical group analysis, the Raman spectrum of this crystal contains 18 vibrational modes ($8A_g + 10B_g$) [5]. In the Cartesian coordinate system whose y axis is parallel to the second-order axis C_2, the Raman tensors for this structure have the form

$$\begin{vmatrix} \alpha_{xx} & \cdot & \alpha_{xz} \\ \cdot & \alpha_{yy} & \cdot \\ \alpha_{zx} & \cdot & \alpha_{zz} \end{vmatrix} \text{ for } A_g, \quad \begin{vmatrix} \cdot & \alpha_{xy} & \cdot \\ \alpha_{yx} & \cdot & \alpha_{yz} \\ \cdot & \alpha_{zy} & \cdot \end{vmatrix} \text{ for } B_g.$$

The crystallographic axes of the single crystal were oriented as follows: $a||x$, $b||y$, $c||z$. The polarised Raman spectra excited by an argon laser with $\lambda = 488.0$ nm were recorded in the backscattering geometry on a SPEX Ramalog 1403 spectrometer with a spectral resolution of 0.6 cm^{-1}. Since the angle β in the monoclinic structure of $ZnWO_4$ is almost 90° [4], we had no problems related to the manifestation of birefringence when adjusting the sample. Figure 1a shows the polarised Raman spectra in the scattering geometries corresponding to all the six Raman tensor components for the $ZnWO_4$ crystal. This allowed us to reliably identify the frequencies of the total set of vibrational modes $8A_g + 10B_g$. The frequencies of vibrational modes recorded by us in the Raman spectra of the $ZnWO_4$ crystal are listed in Table 1. In particular, we managed to separate the closely spaced lines with the A_g and B_g symmetries in the frequency ranges 180 – 200 and 260 – 280 cm^{-1} (Fig. 1b).

Vibrations in the $ZnWO_4$ structure were also previously identified in [5]. However, the authors of [5] used polycrystalline samples unsuitable for polarisation studies, and the symmetry of vibrational modes was determined based on model calculations. Because of this, in [5], not all the Raman-active vibrational modes of $ZnWO_4$ were recorded and, in addition, the symmetry of some vibrations was identified incorrectly.

Figure 1a demonstrates that of interest for SRS conversion is the most intense line with the A_g symmetry at a frequency of 906 cm^{-1}. From the spontaneous Raman spectra, using the method of [6 – 8], we determined the integral (σ_{int}) and peak (σ_{peak}) cross sections of this line, as well as its width $\Delta\nu_R$, which is inversely proportional to the dephasing time T_2 of the Raman-active vibration.

These spectroscopic parameters for $ZnWO_4$ and

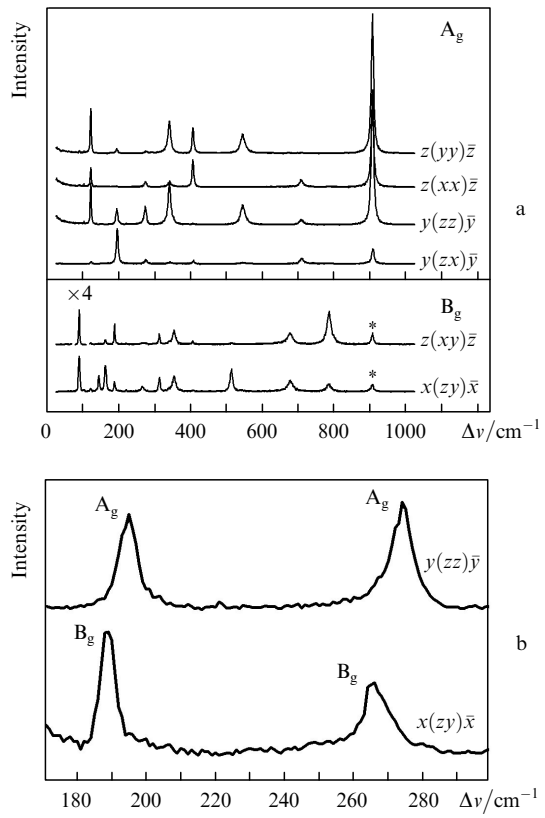

Figure 1. Polarised Raman spectra of the zinc tungstate single crystal in the frequency regions 0–1000 cm^{-1} (a) and 170–300 cm^{-1} (b) at a temperature of 300 K. The asterisks indicate the vibrations forbidden in the given scattering geometry.

Table 1. Vibrational frequencies in the Raman spectra of $ZnWO_4$ at 300 K.

Vibrational frequencies/cm^{-1}	
A_g	B_g
	91
123	
	145
	166
	190
195	
	267
275	
	314
342	
	355
408	
	515
544	
	680
708	
	785
906	

$KGd(WO_4)_2$ crystals are listed in Table 2. Depending on the relation between the laser pump pulse duration T_p and the dephasing time T_2, either stationary or nonstationary SRS can dominate. The SRS gain efficiency decreases as the process changes from stationary to nonstationary.

The KGW crystal is known as the most efficient material for SRS of picosecond pules owing to the short dephasing time. For this crystal, T_2 is about 2 ps and SRS retains the stationary character even under picosecond pumping with $T_p = 10 - 20$ ps. The maximum σ_{int} and σ_{peak} of the SRS active mode for the $ZnWO_4$ crystal correspond to the excitation polarisation $\boldsymbol{E}||b$. The cross section σ_{int} for $ZnWO_4$ and KGW crystals are close to each other, while the cross sections σ_{peak} are different, which is caused by the different widths of the Raman lines: the linewidth $\Delta\nu_R = 7.5\ cm^{-1}$ for the $ZnWO_4$ exceeds the linewidth $\Delta\nu_R = 5.4\ cm^{-1}$ for the KGW by a factor of 1.4. Correspondingly, the cross section σ_{peak} for $ZnWO_4$ is by a factor of 1.4 smaller than that for KGW crystals. The stationary SRS gain g is determined by the peak cross section, because of which this coefficient for the $ZnWO_4$ crystal should be expected to be lower than for KGW. However, for short pulses, whose duration is comparable with T_2, SRS in $ZnWO_4$ is closer to stationary and, hence, is more efficient.

3. SRS in $ZnWO_4$ crystals

SRS in $ZnWO_4$ crystals is easily observed under picosecond laser excitation in the near IR spectral region [9]. As we showed in [10], in the case of high-power picosecond excitation in the green spectral region, the SRS threshold in $ZnWO_4$ can hardly be achieved because of the occurrence of competing nonlinear two-photon absorption. The latter increases the SRS threshold because it significantly restricts the laser radiation power in the crystal due to a strong induced absorption at the pump wavelength.

In [11], we proposed and demonstrated a method for measuring the SRS gain by measuring the SRS threshold upon pumping by a train of picosecond laser pulses with varying intensity. Comparing the measured data with the theoretical results [12], we can determine the SRS gains for both stationary and nonstationary processes. In the present work, we measure the SRS threshold energy for $ZnWO_4$ and KGW crystals using the technique described in [11].

SRS in the crystals was excited by picosecond pulses of a passively mode-locked laser based on a Nd : YLF crystal. The laser emitted trains of pulses with the duration $T_p = 22$ ps at the wavelength $\lambda = 1047$ nm (Fig. 2a). The pulse train consisted of about 20 pulses with continuously varying amplitude. We focused the single-mode laser radiation into the nonlinear crystal by a spherical long-focus ($f = 70$ cm) mirror and measured the temporal, energy, and spectral parameters of radiation. The SRS in the $ZnWO_4$ single crystal 18 mm long was excited along the c axis of the monoclinic structure. The linear pump polarisation vector $\boldsymbol{E}$ coincided with the b axis (C_2) in one case and with the a axis

Table 2. Spectroscopic parameters of SRS-active modes in $ZnWO_4$ and KGW crystals, normalised pump energy thresholds $E_{th}L$, and SRS gains g.

Crystal	ν_R/cm^{-1}	$\Delta\nu_R/cm^{-1}$	Excitation direction and polarisation	σ_{int} (arb. units)	σ_p (arb. units)	$E_{th}L$ (arb. units)	$g/cm\ GW^{-1}$
$ZnWO_4$	906	7.5	$\boldsymbol{k}||c, \boldsymbol{E}||b$	146	23	1.3	3.9
			$\boldsymbol{k}||c, \boldsymbol{E}||a$	88	14	1.6	3.2
KGW	901	5.4	$\boldsymbol{k}||b, \boldsymbol{E}||a$	150	31	1	5.1

in the other case. For comparison, we measured the SRS parameters in a 10-mm-long $KGd(WO_4)_2$ crystal upon excitation of the 901-cm^{-1} resonance. In this case, the SRS was excited along the b axis and the excitation polarisation vector coincided with the a axis.

SRS in the $ZnWO_4$ crystal occurs at the 906-cm^{-1} Stokes component. Figure 2a presents the oscillograms of the pump and SRS pulses for one laser shot. The SRS pulse train is much shorter than the pump pulse train. One can clearly see the SRS start and termination. Plotting the dependences of the SRS pulse energy E_s on the pump pulse energy E_p (Fig. 2b), we can determine the threshold pump pulse energy E_{th}. These dependences were obtained at a relatively weak pumping in the absence of cascade generation of higher Stokes components. For comparison, Fig. 2b shows the SRS (the 901-cm^{-1} Stokes component) efficiency for a $KGd(WO_4)_2$ crystal under the same conditions.

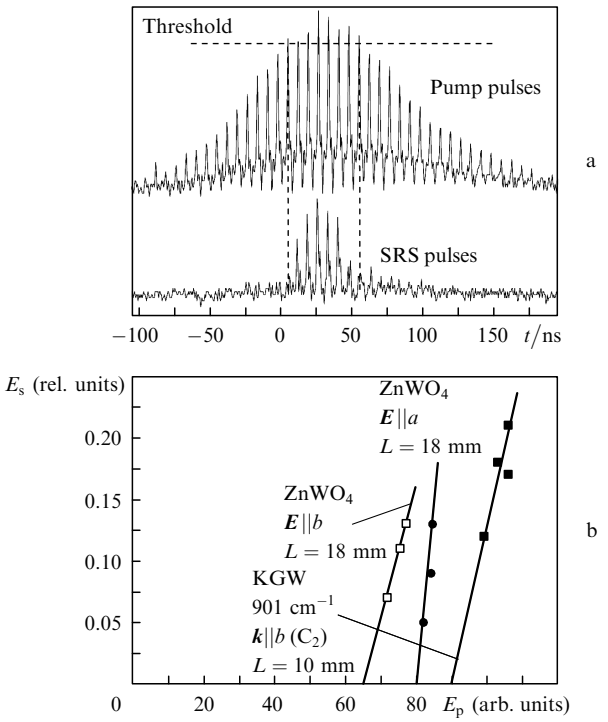

Figure 2. Oscillograms of the pump and SRS pulses in the $ZnWO_4$ crystal (a) and dependences of the output SRS pulse energy on the pump pulse energy for $ZnWO_4$ and KGW crystals (b).

In the stationary SRS regime, when the pump pulse duration considerably exceeds the dephasing time ($T_p/T_2 \gg 1$), the gain increment at constant pumping is directly proportional to the pump intensity I_p and the nonlinear interaction length L, $G_0 = gI_pL$, where g is the stationary gain. The threshold increment G_0 is achieved at the intensity $I_{th} = E_{th}/(\tau S)$ corresponding to E_{th} (S is the beam cross section area and τ is the pump pulse duration). The parameter $E_{th}L$ characterises the SRS gain. Owing to the large length of the $ZnWO_4$ crystal (18 mm), its E_{th} turned out to be lower than that for the KGW crystal (10 mm long). At the same time, the normalised energy threshold $E_{th}L$ for the $ZnWO_4$ crystal for the pump polarisation $\boldsymbol{E}||b$ exceeds the normalised threshold for the KGW crystal by a factor of 1.3, and, correspondingly, the SRS gain for $ZnWO_4$ is smaller than that for KGW. The ratio of the normalised thresholds $E_{th}L$ for these crystals was found to be close to the ratio of their peak Raman cross sections (1.4), i.e., the gains in both crystals are determined by the peak Raman cross sections. This points to the stationary SRS in both crystals in the case of excitation by 22-ps pulses.

Using the measured normalised threshold energies $E_{th}L$ and the previously measured coefficient $g = 5.1$ cm GW^{-1} for the KGW crystal [11], we determined the stationary SRS gains in $ZnWO_4$ for two excitation polarisations (see Table 2). These coefficients vary from 3.9 to 3.2 cm GW^{-1} depending on the excitation polarisation. The SRS gains for $ZnWO_4$ crystals are lower than for other oxide crystals [11]. Nevertheless, the $ZnWO_4$ crystal, which has a short optical dephasing time ($T_2 = 1.4$ ps), seems to be promising for obtaining picosecond SRS pulses in the near-IR spectral region [13].

Acknowledgements. This work was supported by the Grant of the President of the Russian Federation for the State Support of Young Russian Scientists (Grant No. MK-816.2010.2) and by the Russian Foundation for Basic Research (Grant No. 10-02-00254-a).

References

1. Basiev T.T. *Usp. Fiz. Nauk*, **169**, 1149 (1999).
2. Basiev T.T., Osiko V.V., Prokhorov A.M., Dianov E.M. *Topics Appl. Phys*,. **89**, 351 (2003).
3. Basiev T.T., Powell R.C., in *Handbook of Laser Technology and Applications* (Bristol, Philadelphia: IOP Publ., 2004) Ch. B 1.7, p. 469.
4. Filippenko O.S., Pobedimskaya U.A., Belov N.V. *Kristallografiya*, **18**, 163 (1968).
5. Fomichev V.V., Kondratov O.I. *Spectrochim. Acta*, **50A**, 1113 (1994).
6. Basiev T.T., Sobol A.A., Zverev P.G., Osiko V.V., Powell R.C. *Appl. Opt*., **38**, 594 (1999).
7. Basiev T.T., Sobol A.A., Zverev P.G., Ivleva L.I., Osiko V.V., Powell R.C. *Opt. Mater*., **11**, 307 (1999).
8. Basiev T.T., Sobol A.A., Voron'ko Yu.K., Zverev P.G. *Opt. Mater*., **15**, 205 (2000).
9. Kaminskii A.A., Eichler H.J., Ken-ichi Ueda, et al. *Appl. Opt*., **38**, 4533 (1999).
10. Lukanin V.I., Chunaev D.S., Karasik A.Ya. *Pis'ma Zh. Eksp. Teor. Fiz*. **91**, 615 (2010).
11. Basiev T.T., Zverev P.G., Karasik A.Ya., Osiko V.V., Sobol A.A., Chunaev D.S. *Zh. Eksp. Teor. Fiz*., **126**, 5 (2004).
12. Carman R.L., Shimizu F., Bloembergen N., et al. *Phys. Rev. A*, **2**, 60 (1970).
13. Chunaev D.S., Karasik A.Ya. *Laser Phys*., **16**, 1668 (2006).